Journal of Cerebral Blood Flow & Metabolism (2011) 31, 671–679

www.jcbfm.com

Framingham cardiovascular risk profile correlates with impaired hippocampal and cortical vasoreactivity to hypercapnia

Lidia Glodzik[1], Henry Rusinek[2], Miroslaw Brys[1], Wai H Tsui[1], Remigiusz Switalski[3], Lisa Mosconi[1], Rachel Mistur[1], Elizabeth Pirraglia[1], Susan de Santi[4], Yi Li[1], Alexander Goldowsky[1] and Mony J de Leon[1,5]

[1]*Center for Brain Health, Department of Psychiatry, New York University School of Medicine, New York, New York, USA;* [2]*Department of Radiology, New York University School of Medicine New York, New York, USA;* [3]*East Tennessee State University, Department of Family Medicine, Johnson City, Tennessee, USA;* [4]*Bayer HealthCare, Montville, New Jersey, USA;* [5]*Nathan Kline Institute Orangeburg, New York, USA*

Vascular risk factors affect cerebral blood flow (*CBF*) and cerebral vascular reactivity, contributing to cognitive decline. Hippocampus is vulnerable to both Alzheimer's disease (AD) pathology and ischemia; nonetheless, the information about the impact of vascular risk on hippocampal perfusion is minimal. Cognitively, healthy elderly (NL = 18, 69.9 ± 6.7 years) and subjects with mild cognitive impairment (MCI = 15, 74.9 ± 8.1 years) were evaluated for the Framingham cardiovascular risk profile (*FCRP*). All underwent structural imaging and resting *CBF* assessment with arterial spin labeling (ASL) at 3T magnetic resonance imaging (MRI). In 24 subjects (NL = 17, MCI = 7), *CBF* was measured after a carbon dioxide rebreathing challenge. Across all subjects, *FCRP* negatively correlated with hippocampal ($\rho = -0.41$, $P = 0.049$) and global cortical ($\rho = -0.46$, $P = 0.02$) vasoreactivity to hypercapnia (VR_h). The *FCRP*–VR_h relationships were most pronounced in the MCI group: hippocampus ($\rho = -0.77$, $P = 0.04$); global cortex ($\rho = -0.83$, $P = 0.02$). The *FCRP* did not correlate with either volume or resting *CBF*. The hippocampal VR_h was lower in MCI than in NL subjects ($Z = -2.0$, $P = 0.047$). This difference persisted after age and *FCRP* correction ($F_{[3,20]} = 4.6$, $P = 0.05$). An elevated risk for vascular pathology is associated with a reduced response to hypercapnia in both hippocampal and cortical tissue. The VR_h is more sensitive to vascular burden than either resting *CBF* or brain volume.

Journal of Cerebral Blood Flow & Metabolism (2011) **31,** 671–679; doi:10.1038/jcbfm.2010.145; published online 15 September 2010

Keywords: atherosclerosis; cerebral blood flow; cognitive impairment; hippocampus; MRI

Introduction

Multiple imaging modalities corroborate the relationship between vascular risk factors and deficits in resting cerebral blood flow (*CBF*) (Claus *et al*, 1996; Novak *et al*, 2006; Selim *et al*, 2008; Beason-Held *et al*, 2007). Similarly, atherosclerosis risk factors impair vascular response to hypercapnia (Groschel *et al*, 2007; Settakis *et al*, 2003), as evidenced by Doppler studies.

Correspondence: Dr L Glodzik, Center for Brain Health, Department of Psychiatry, New York University School of Medicine, 145 East 32nd Street, New York, 10016 NY, USA.
E-mail: lidia.glodzik@nyumc.org
This study was supported by the following grants: NIH-NIA AG08051, AG12101, AG022374, and the Alzheimer's Association Grants: IIRG-08-91038 and NIRG-09-132490.
Received 14 April 2010; revised 7 July 2010; accepted 11 July 2010; published online 15 September 2010

Resting *CBF* reductions are also well documented by single photon emission tomography in individuals with mild cognitive impairment (MCI) (Staffen *et al*, 2006; Hirao *et al*, 2005; Caroli *et al*, 2007). Furthermore, both *CBF* reduction (Hirao *et al*, 2005; Caroli *et al*, 2007; Hansson *et al*, 2009; Johnson *et al*, 1998; Kitagawa *et al*, 2009; Chao *et al*, 2010) and deficits in the reactivity of cerebral vessels to hypercapnia (vasoreactivity to hypercapnia (VR_h)) forecast cognitive decline (Silvestrini *et al*, 2006). It has been thus proposed that preexisting vascular risk factors mechanistically contribute to cognitive deterioration by directly compromising cerebral blood supply, especially in the states of increased demand.

Although many reports substantiate the link between risks for atherosclerosis and blood flow at a global cerebral or lobar level (Claus *et al*, 1996; Novak *et al*, 2006; Selim *et al*, 2008; Groschel *et al*, 2007; Settakis *et al*, 2003), there is only a limited information about the influence of these factors

on *CBF* in structures directly related to memory function. Hippocampus is a major anatomical substrate of memory (Eichenbaum, 2004; Shapiro, 2001), and its structural and functional abnormalities predict Alzheimer's disease (AD) (Glodzik-Sobanska *et al*, 2005; Mosconi, 2005). As hippocampal cornu ammonis sector1 is highly sensitive to both AD pathology and ischemia (Zarow *et al*, 2005), the presence of vascular risk can strongly compound on AD-related damage. It hence follows that evaluation of the vascular risk–perfusion relationship in the hippocampus of nondemented individuals could be informative in assessing the contribution of atherosclerosis to cognitive decline. Although hypertension-related deficits in resting hippocampal *CBF* were previously described (Dai *et al*, 2008; Beason-Held *et al*, 2007), there are no hippocampal VR_h data available. Moreover, previously used statistical parametric mapping procedures do not provide an accurate assessment of small structures like hippocampus because of smoothing and likely mismatch of coordinates (Mosconi *et al*, 2005).

Arterial spin labeling (ASL) is a noninvasive magnetic resonance imaging (MRI) perfusion technique in which labeled arterial blood is used as a tracer. The ASL does not involve radiation exposure or exogenous contrast material (Buxton, 2005). Unlike positron emission tomography or single photon emission tomography, ASL is capable of direct *CBF* examination at spatial resolution sufficient to resolve small structures of interest. Yet, hippocampal MRI perfusion studies are still challenging, as the often used ASL techniques based on echo-planar imaging may suffer from susceptibility artifacts. This can be particularly detrimental for regions located in the proximity of bone and sinuses. Moreover, conventionally used 64×64 echo-planar imaging matrix does not allow one to separate hippocampus from adjacent large vessels, including circle of Willis. To overcome these shortcomings, we used ASL based on true fast imaging in steady-precession (TrueFISP) sequence (Boss *et al*, 2007; Rusinek *et al*, 2010).

We compared perfusion characteristics in elderly subjects with normal cognition or MCI and investigated the hypothesis that an elevated Framingham cardiovascular risk profile (*FCRP*) score (NIH Publication No.02-5125 & US Department of Health and Human Services, 2002) is associated with a hemodynamic impairment of the hippocampus and neocortex.

Materials and methods

Subjects

In all, 33 individuals (age 71.2 ± 7.6 years, range 59 to 88 years, 58% women) were studied at the NYU School of Medicine, Center for Brain Health and Alzheimer's Disease Center. All were active participants in longitudinal studies of aging and dementia. All gave written informed consent to an institutional review board-approved protocol. Subjects received medical, neurologic, psychiatric, neuropsychological, laboratory and MRI examinations. Patients with confounding brain conditions, for example tumor, depression, significant metabolic diseases, and neocortical infarction, were excluded. Also excluded were patients with contraindications for MRI scanning. The clinical assessment included a semistructured interview based on the Brief Cognitive Rating Scale, Global Deterioration Scale score (GDS) (Reisberg and Ferris, 1988), and Mini-Mental State Examination (MMSE) (Folstein, 1983). All subjects were diagnosed as normal (NL; GDS = 1 or 2, $n = 18$) or MCI (GDS = 3, $n = 15$) (Reisberg *et al*, 1993). GDS = 1 indicated no subjective memory complaint, and GDS = 2 indicated awareness of memory change over the lifespan, in the absence of objective evidence of memory or functional problems on clinical interview. The MCI was defined as global functioning in the no-dementia range and evidence of cognitive impairment on clinical interviews (Reisberg *et al*, 1993). All diagnoses were assigned at a consensus case conference.

Cardiovascular risk was determined with the Framingham risk equation (NIH Publication No.02-5125 & US Department of Health and Human Services, 2002), which accounts for age, gender, systolic blood pressure, antihypertensive treatment, smoking, total cholesterol, and HDL levels. For each subject, we computed a score representing the percentage risk for coronary heart disease in the next 10 years.

Imaging

Brain imaging was performed within 6.7 ± 7.0 months of the clinical assessment. Imaging was performed on a 3T Siemens TIM Trio scanner equipped with high-performance gradient coils (45 mT/m maximum gradient strength, 200 mT/m per milliseconds slew rate) and a 12-element head coil.

Structural imaging: High-resolution T1-weighted magnetization-prepared rapid gradient-echo (MPRAGE) images were acquired with the following parameters: repetition time (*TR*)/echo time (*TE*)/inversion time (*TI*) = 2300/2.8/1100 milliseconds, flip angle (FA) = 9°, 208 1 mm slices, bandwidth (BW) = 220 Hz/pixel, field of view (FOV) = 25 cm, isotropic voxel size = $1 \times 1 \times 1$ mm^3, 5 minutes 4 seconds acquisition time.

White matter hyperintensities: The fluid attenuated inversion recovery (FLAIR) images were available for 90% of the subjects. They were acquired during a separate session on average within 16 months of the ASL study. They were used to assess the extent of periventricular white matter hyperintensities (PWMH) and deep white matter hyperintensities (DWMH) on the 0 to 3 Fazekas scale (Fazekas *et al*, 1987).

Perfusion imaging: A pulsed ASL sequence which combines a flow-sensitive alternating inversion-recovery (FAIR) labeling scheme with segmented TrueFISP readout was used. Imaging parameters are: *TR*/*TE*/*TI* = 3.4/1.7/

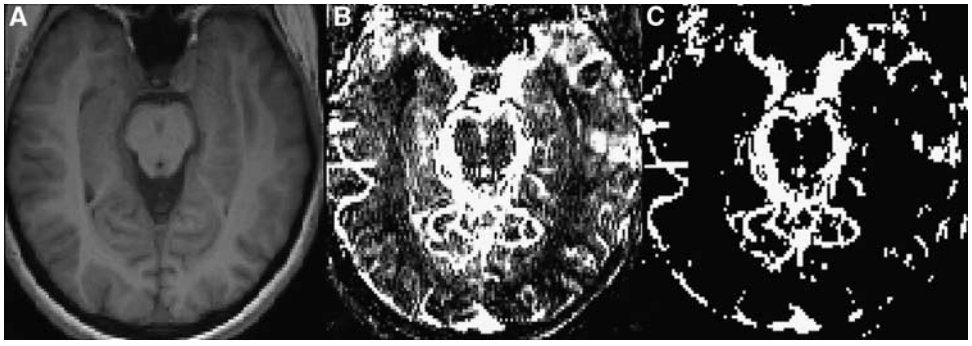

Figure 1 (**A**) Anatomical axial T1 image of the brain (section through the hippocampus), (**B**) flow image with overlaid vessels, (**C**) vessels separated from tissue flow image.

1200 milliseconds, flip angle = 50°, bandwidth = 975 Hz/pixel, 256×168 matrix, 171 phase-encoding steps, $30 \times 19.7\,cm^2$ FOV, voxel size = $1.2 \times 1.2 \times 6\,mm^3$, number of excitations (*NEX*) = 8. The TrueFISP acquisition is repeated without the FAIR preparation (with *NEX* = 4) to estimate the steady-state magnetization M_0. Total acquisition time was approximately 2:40 minutes (Rusinek *et al*, 2010). Selecting acquisition plane included (1) selecting the sagittal slice through the long axis of the right hippocampus, (2) drawing the line segment H–H' through this axis of the right hippocampus, and (3) adjusting the axial plane by rotating it about the H–H' axis to encompass the left hippocampus (Figure 1).

Imaging the Vasoreactivity to Hypercapnia

To estimate the VR_h, blood CO_2 level was increased using a rebreathing protocol. Subjects were asked to breathe through a mouthpiece and a respiratory tube. The rebreathing apparatus included a high efficiency particulate air (HEPA) bacterial/viral filter and a standard gas-anesthesia tube (VitalSigns, Totowa, NJ, USA) of 35 mm diameter and a custom-adjusted length. Nose was clamped to force inspiration of partially exhaled air. The protocol was demonstrated to the patients who practiced rebreathing during a 15-minute training session, before the MRI examination. Oxygen saturation, heart rate, and CO_2 content in the expired air were monitored in the training room and in the scanner using a multigas monitor (Medrad (R) 9500, Warendale, PA, USA). Expired air was sampled continuously by an infrared capnometer via a 3-m long cannula.

Postprocessing

Segmentation of structural images: Segmentation of high-resolution MPRAGE images to gray matter (GM), white matter (WM), and cerebrospinal fluid volumes was performed using automated statistical parametric mapping (SPM2) procedures (Ashburner and Friston, 2000). Left and right hippocampus were manually outlined on reformatted coronal MPRAGE images (Convit *et al*, 1997).

Image coregistration: As both perfusion and MPRAGE images were collected during one short session, coregistration of perfusion and structural images was based on 'Image Orientation Patient' and 'Image Position Patient' digital imaging and communications in medicine (DICOM) parameters preserved by the scanner console. The accuracy of coregistration was then checked individually.

Calculation of Blood Flow

Calculation was based on the following equation:

$$CBF = \frac{\Delta M \lambda e^{TI/T_1}}{2\alpha TI\, M_0} = g\Delta M$$

where ΔM stands for the adjusted difference between tagged and untagged data, λ is the blood–tissue water partition coefficient (assumed 0.9 mL/g), α is the inversion efficiency, *TI* is the inversion delay (1200 milliseconds), and M_0 the steady-state magnetization. Since at *TI* = 1200 milliseconds, most of the magnetization remains in the blood (Buxton, 2005), the relaxation time of the arterial blood T_1 = 1930 milliseconds (Stanisz *et al*, 2005) was uniformly used across all regions. There was no smoothing of ASL images. The following steps were subsequently applied:

1. Calibration of tagged and untagged signal with WM: We used the WM to adjust ΔM. This correction is needed due to the violation of the ASL measurement assumption (equal signal of tagged and untagged image in the absence of flow) by FAIR preparation pulses. Given that WM perfusion is significantly lower than cortical flow (Law *et al*, 2000), we used the signal difference measured in WM ΔM_{WM} to adjust *CBF*, where *g* is the factor from the 'standard ASL equation' (as above).

$$CBF = g(\Delta M - \Delta M_{WM}) + CBF_{WM}$$

On the basis of prior studies, we assume 25 mL per 100 g per minute for CBF_{WM} (Law *et al*, 2000).

2. Correction for atrophy and tissue inhomogeneity: TrueFISP images were coregistered with MPRAGE volumes (GM and WM) and regions of interest (ROIs). Each voxel in each ROI is then examined in relation to its SPM2-derived GM and WM. For cortical and hippocampal ROIs (Figure 2), voxels were deleted if their probability of being GM was < 75%. Similarly, WM voxels were not included if their probability of being WM was < 75%.

3. Exclusion of blood vessels: To avoid error introduced by labeled arterial blood within the ROIs, all voxels with *CBF* > 150 mL per 100 g per minute were deemed to contain

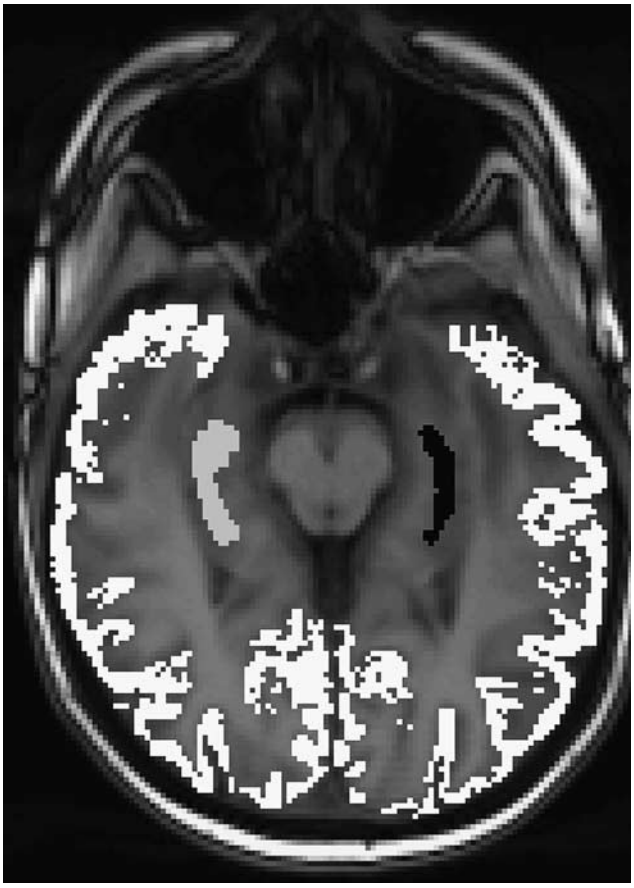

Figure 2 Cortical and hippocampal regions of interest (ROIs) overlaid on arterial spin labeling (ASL) image.

large blood vessels and were excluded from ROIs. This is possible due to distinctive ability of segmented TrueFISP to visualize blood vessels of diameter larger than ~1 mm (Figure 1).

Sampling of regional cerebral blood flow: This was performed using manually (hippocampus) or automatically SPM-segmented (global GM) volumes, coregistered with the TrueFISP images (Figure 2). The *CBF* was calculated for cortical GM (an integral of all cortical regions visible on the imaged slice), the right and left hippocampus separately (Figure 2).

Calculating the response to CO_2: The VR_h response to an increase in blood CO_2 was calculated as:

$$VR_h = ((CBF_{CO_2} - CBF_{rest})/CBF_{rest}) \times 100)/\Delta CO_2$$

where CBF_{CO2} indicates *CBF* calculated during the session when subjects breathed through a respiratory tube, CBF_{rest} indicates *CBF* calculated during the imaging session without the tube; ΔCO_2 indicates the difference in end tidal CO_2 between the two sessions.

Statistical Analysis

Demographic measures were examined using *t*-test for continuous variables and χ^2 for categorical variables. Between-group comparisons of global volumes, *CBF* and *VR* data were performed with *t*-tests. When covariates were necessary, analysis of covariance was used. Correlations between variables were examined with Spearman coefficient. When accounting for confounding variables was necessary, partial correlations were used. Normality was checked using the Shapiro–Wilk test. When the data did not meet the assumptions of normality, the Mann–Whitney *U*-test was used to compare groups (*Z* values are given). When covariates were needed, dependent variables were converted to ranks and analyzed in analysis of covariance models. All volumes (global GM, hippocampus left, right, and averaged) were divided by total intracranial volume determined by manual tracing (Convit *et al*, 1997) and presented as intracranial volume percentage. The *CBF* and VR_h data for the right and left hippocampus were analyzed separately and averaged. Analyses were performed with SPSS 16, Chicago, IL, USA, with *P* values <0.05 declared statistically significant.

Results

Normal Versus Mild Cognitive Impairment

General description: Characteristics of both groups are presented in Table 1. The MCI subjects had lower MMSE scores ($Z=-2.3$, $P=0.03$) and tended to be older ($t=-1.8$, $P=0.08$) than controls. After accounting for age, MMSE difference was no longer significant. Although, the groups did not differ in *FCRP*, the percentage of subjects with high-*FCRP* score (>10%) was significantly increased in the MCI group (53% versus 11%, $\chi^2=6.9$, $P=0.009$).

Volumetrics: The groups did not differ in hippocampal or cortical volumes (age corrected).

Cerebral blood flow: The *CBF* did not differ between NL and MCI groups in any examined region (age corrected) (Table 1).

Cerebral vasoreactivity to hypercapnia: In all, 24 subjects (NL = 17 and MCI = 7; Table 2) underwent the rebreathing challenge. Overall, the mean CO_2 increase was 6.8 ± 1.7 mm Hg. The mean increase in global cortical, right hippocampal, left, and averaged hippocampal *CBF* was 2.7, 3.3, 3.1, and 3.2 mL per 100 g per minute, respectively. The nine subjects with no VR_h data did not differ in age, gender, or *FCRP* score from subjects with VR_h data available, they had, however, lower MMSE score (26.7 ± 2.7 versus 29.0 ± 1.1; $Z=-2.6$, $P<0.05$). The MCI group had lower average hippocampal VR_h than NL subjects ($Z=-2.0$, $P=0.047$). This association still tended to be significant after age and *FCRP* correction ($F_{[3,20]}=4.6$, $P=0.05$).

Framingham Cardiovascular Risk Profile and Cerebral Perfusion

General description: The mean *FCRP* score was $8.7\% \pm 6.7\%$. The *FCRP* score correlated with age

Table 1 Study variables by cognitive diagnosis (NL versus MCI)

Variable	*NL* (n = *18*)	*MCI* (n = *15*)	P
Age	69.9 ± 6.7	74.9 ± 8.1	0.07
Gender (% female)	56	60	NS
MMSE	29.2 ± 1.0	27.5 ± 2.4	0.02
FCRP	7.4 ± 4.3	10.3 ± 8.6	NS
% With FCRP > 10%	11	53	0.009
% With CVD	0	7	NS
% With LVH	6	20	NS
% With DB	0	7	NS
PWMH score	(n = 17) 0.90 ± 0.85	(n = 17) 1.40 ± 0.65	NS
DWMH score	(n = 13) 0.90 ± 0.70	(n = 13) 0.80 ± 0.60	NS
Baseline CO_2 (mm Hg)	39.5 ± 3.3	39.3 ± 4.9	NS
Volume (% of ICV)			
GM	54 ± 3	53 ± 4	NS
Right hippocampus	0.20 ± 0.02	0.18 ± 0.03	NS
Left hippocampus	0.20 ± 0.03	0.18 ± 0.03	NS
Averaged hippocampus	0.20 ± 0.02	0.18 ± 0.03	NS
CBF (mL per 100 g per minute)			
Global cortical	60.4 ± 7.6	58.2 ± 11.3	NS
Right hippocampus	58.1 ± 9.1	58.8 ± 15.3	NS
Left hippocampus	57.1 ± 11.6	55.7 ± 14.6	NS
Averaged hippocampus	57.6 ± 8.8	57.3 ± 12.7	NS

CBF, cerebral blood flow; CVD, cardiovascular disease; DB, diabetes mellitus; DWMH, deep white matter hyperintensities; FCRP, Framingham cardiovascular risk profile; GM, gray matter; ICV, intracranial volume; LVH, left ventricular hypertrophy (on ECG); MCI, mild cognitive impairment; MMSE, Mini-Mental State Examination; PWMH, periventricular white matter hyperintensities.
Values represent mean ± s.d.
PWMH and DWMH were measured on the 0–3 Fazekas scale (Fazekas *et al*, 1987).

Table 2 Study variables by cognitive diagnosis (NL versus MCI) in the groups with VR_h data available

Variable	*NL* (n = *17*)	*MCI* (n = *7*)	P
Age	69.8 ± 6.9	73.4 ± 8.2	NS
Gender (% female)	53	71	NS
MMSE	29.2 ± 1.0	28.6 ± 1.4	NS
FCRP	7.6 ± 4.4	8.0 ± 5.4	NS
% With FCRP > 10%	12	57	0.02
% With LVH	6	0	NS
PWMH score	(n = 16) 0.90 ± 0.85	(n = 6) 1.20 ± 0.40	NS
DWMH score	(n = 16) 0.90 ± 0.70	(n = 6) 0.70 ± 0.50	NS
Baseline CO_2 (mm Hg)	39.2 ± 3.1	38.7 ± 5.9	NS
mean CO_2 increase (mm Hg)	7.1 ± 1.8	6.2 ± 1.4	NS
Volume (% of ICV)			
GM	54 ± 3	54 ± 3	NS
Right hippocampus	0.20 ± 0.02	0.19 ± 0.03	NS
Left hippocampus	0.20 ± 0.03	0.20 ± 0.03	NS
Averaged hippocampus	0.20 ± 0.02	0.19 ± 0.03	NS
CBF (mL per 100 g per minute)			
Global cortical	60.6 ± 7.7	57.8 ± 4.2	NS
Right hippocampus	58.1 ± 9.4	60.3 ± 13.4	NS
Left hippocampus	57.4 ± 11.8	55.3 ± 7.8	NS
Averaged hippocampus	57.8 ± 9.0	57.8 ± 9.4	NS
VR_h (% ΔCBF/1 mm Hg CO_2)			
Global cortical	1.0 ± 1.5	0.31 ± 1.2	NS
Right hippocampus	1.4 ± 2.7	0.23 ± 2.5	NS
Left hippocampus	1.5 ± 3.3	−0.22 ± 1.5	0.099
Averaged hippocampus	1.4 ± 2.7	−0.05 ± 1.7	0.047

CBF, cerebral blood flow; DWMH, deep white matter hyperintensities; FCRP, Framingham cardiovascular risk profile; GM, gray matter; ICV, intracranial volume; LVH, left ventricular hypertrophy (on ECG); MCI, mild cognitive impairment; MMSE, Mini-Mental State Examination; PWMH, periventricular white matter hyperintensities; VR_h, vasoreactivity to hypercapnia.
Values represent mean ± s.d.
None of the subjects in the subset had diabetes mellitus or cardiovascular disease.
PWMH and DWMH were measured on the 0–3 Fazekas scale (Fazekas *et al*, 1987).

in the entire group ($\rho = 0.46$, $P = 0.007$) and in the MCI subjects ($\rho = 0.61$, $P = 0.02$). The *FCRP* did not correlate with any examined brain volumes in the entire group, nor in NL or MCI subgroups (age corrected). The *FCRP* correlated with PWMH ($\rho = 0.48$, $P < 0.01$) but not DWMH.

Cerebral blood flow: In the whole group, *FCRP* score did not correlate with *CBF* in any region. Similarly, no correlations were found in NL or MCI groups (age corrected).

Cerebral vasoreactivity to hypercapnia: In the entire group, the average hippocampal VR_h was related to *FCRP* ($\rho = -0.41$, $P = 0.049$). Global cortical VR_h also correlated with *FCRP* ($\rho = -0.46$, $P = 0.02$). Further analyses revealed that in the MCI subjects, *FCRP* was strongly related to hippocampal ($\rho = -0.77$, $P = 0.04$) and global cortical VR_h ($\rho = -0.83$, $P = 0.02$) (Figure 3). Relationships in the NL group were weaker with ($\rho = -0.25$, $P = 0.30$) for the average hippocampal and ($\rho = -0.45$, $P = 0.07$) for global cortical VR_h, respectively. Cortical VR_h was also associated with PWMH ($\rho = -0.45$, $P = 0.04$). There was also a similar trend for PWMH and hippocampal VR_h ($\rho = -0.31$, $P = 0.16$). After correcting for PWMH, the relationship between *FCRP* and VR_h was still at the trend level: $\rho = -0.36$, $P = 0.1$ for the cortex; and $\rho = -0.33$, $P = 0.15$ for the hippocampus.

Cerebral Perfusion and Other Measures

Cerebral blood flow: Resting *CBF* was not related to age in any examined region. This was true for the entire group, and within NL and MCI subsets. Regionally, the *CBF* was not related to the brain volumes in the entire groups nor in subsets of NL and MCI subjects. There was no association between resting flow and baseline CO_2 levels, PWMH, or DWMH.

In the entire group, global *CBF* was related to MMSE score ($\rho = 0.40$, $P = 0.027$, age corrected). Additional corrections did not change this association ($\rho = 0.40$, $P = 0.031$, age, gender, and education corrected). When examined within groups, this relationship was found only in MCI subjects ($\rho = 0.52$, $P = 0.045$). In the smaller MCI subgroup, MMSE did not correlate with education or age and did not differ between men and women, thus corrections were not necessary.

Cerebral vasoreactivity to hypercapnia: The VR_h was not related to age, regional brain volumes, or MMSE, in either the entire group or in NL and MCI subgroups.

Discussion

Our study yielded two major findings: (1) cerebral VR_h, as measured with ASL combined with CO_2-rebreathing procedure, was negatively related to the level of cardiovascular risk and (2) VR_h was lower in the hippocampus of MCI subjects as compared with normal controls. Our result expands previous observations from Doppler (Groschel *et al*, 2007) and ASL (Last *et al*, 2007) studies, where decreased response to hypercapnia was found in association with vascular risk factors. Specifically, among all the subjects, both hippocampal and global cortical VR_h were affected by vascular risk, corroborating the contribution of impaired vessel function to the damage of brain regions strategic for cognition.

Our observation of reduced hippocampal VR_h in the MCI group also add to recent results of diminished vessel function in dementia subjects (Silvestrini *et al*, 2006; Vincenzini *et al*, 2007). The

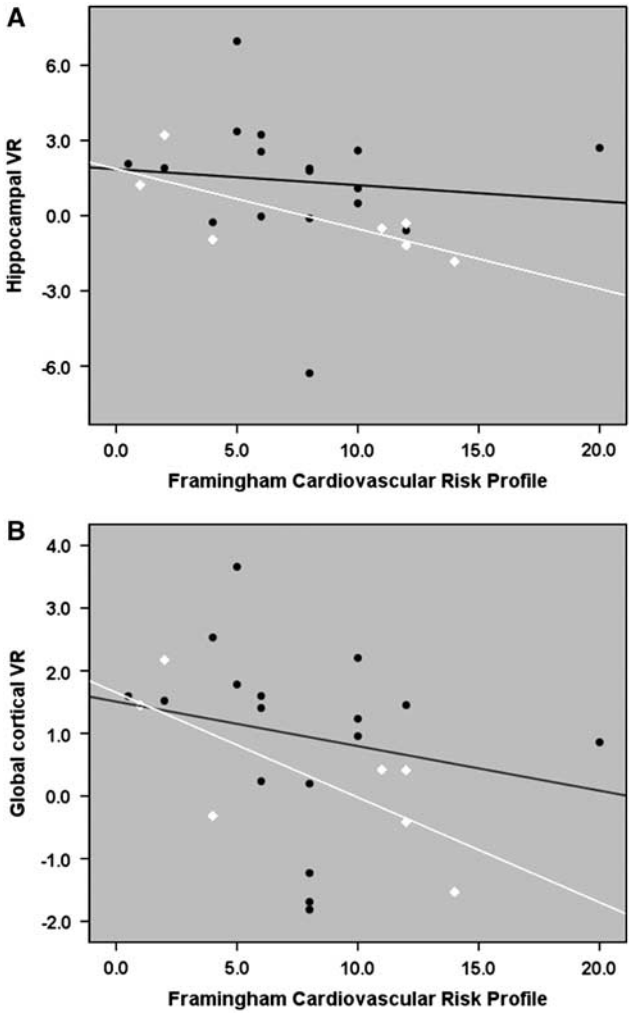

Figure 3 Correlations between Framingham cardiovascular risk profile (*FCRP*) and average hippocampal (**A**) and cortical (**B**) vasoreactivity to hypercapnia (VR_h). The units of VR_h are % ΔCBF/1 mm Hg CO_2. Values on *x* axis represent the percentage risk for coronary heart disease in the next 10 years. Black circles represent normal (NL) subjects and white diamonds represent subjects with mild cognitive impairment (MCI). *CBF*, cerebral blood flow.

FCRP–VR_h association was also found in the MCI subjects. As the number of subjects with increased vascular load (risk > 10%) was higher among MCI subjects, vascular contribution explains at least in part lower VR_h in this group. Recent evidence indicates that patient with hypertension have increased parahippocampal neurofibrillary tangles (Sparks *et al*, 1995), supporting the role of cardiovascular factors in AD. Still, the VR_h difference between NL and MCI persisted after age and *FCRP* score correction. We offer that preexisting vessel impairment (independent of vascular risk, but possibly related to AD) had to be present to potentiate the influence of vascular risk factors on vessel expandability.

Opposite to earlier findings (Dai *et al*, 2009; Staffen *et al*, 2006; Hirao *et al*, 2005; Caroli *et al*, 2007), *CBF* was not different between NL and MCI. Global *CBF* was, however, related to the global cognitive abilities as assessed with MMSE. As MCI subjects were highly functioning (an average MMSE score was above 27) between-group differences in *CBF* were subtle. However, a stronger relationship emerged when cognition–*CBF* relationship was examined across the entire spectrum with MMSE.

Differing from recent reports of reduced resting hippocampal *CBF* (Dai *et al*, 2008; Beason-Held *et al*, 2007) in hypertensive nondemented subjects, we did not observe a relationship between *FCRP* and resting cortical or hippocampal flow. It is noteworthy that in our group, the impact of arthrosclerosis risk factors on vessel dilatation capacity was stronger than their impact on volume or resting *CBF*. One possible explanation for a lack of a relationship between volume or *CBF* and FCRP is low burden of vascular risk in our group. The mean risk for cardiovascular event in our group was 9%, substantially lower than 20% considered being high risk (NIH Publication No.02-5125 & US Department of Health and Human Services, 2002). Conceivably, a mild stage of vascular damage may not affect volumes or *CBF*, and the influence of vascular burden is only evident in a challenge condition. The intrinsically variable nature of resting *CBF*, dependent on such factors as heart rate, hematocrit, subject alertness, and stress level could also explain our negative findings. It is possible that changes in resting perfusion and brain volume reductions occur only in the late stage of atherosclerosis or with more advanced cognitive impairment. We provide, however, a strong evidence for a relationship between vascular burden and a challenge that demands additional blood supply. This is in agreement with previous observations that *FCRP* correlated with impaired endothelium-dependent vasodilatation in the skin (Ijzerman *et al*, 2003).

Decreases in VR_h could reflect hippocampal or cortical volume reductions. However, neither *CBF* nor VR_h in the hippocampus or in the cortex were related to their volumes. In our study, the flow was calculated after exclusion of non-GM voxels, which we believe, accounted for the effects of atrophy and related bias. Thus, the presented values are likely to reflect perfusion of neuronal tissue without partial voluming that is unavoidable in positron emission tomography or single photon emission tomography imaging.

Not surprisingly in our group, vascular burden, VR_h, and PWMH were intercorrelated. The association between reduced response to hypercapnia and WM lesions, especially PWMH, is well known (Bakker *et al*, 1999; Bonoczk *et al*, 2004; Fu *et al*, 2006; Isaka *et al*, 1994). Nonetheless, it still is not completely clear what is a cause what is an effect. Vascular risk factors can be particularly harmful for periventricular WM located in the borderline zone. Conceivably, by compromising blood flow they can contribute to the development of WMH. However, another explanation cannot be ruled out: WMH once present can contribute to the impairment in vascular reactivity, as periventricular zone harbors receptor involved in cerebral vasoregulation (Sandor *et al*, 1986). Our work cannot give a definite answer.

To our knowledge, this is one of the first studies to examine regional VR_h in the hippocampus. The technique we used is less sensitive to susceptibility artifacts than echo-planar imaging (Boss *et al*, 2007), and has improved spatial resolution, enabling separation of vascular signal from tissue blood flow. In addition, the 3T field strength provides a unique advantage for ASL because of longer blood T1 relaxation times, making this technique a promising quantitative approach for *CBF* and *VR* measurement (Petersen *et al*, 2006). Many arteries $\sim$1 mm in diameter can be visualized (Figure 1). Consequently, large vessels can be automatically excluded from tissue ROIs, and no crusher gradient pulse is needed to dephase fast-moving vascular flow. The voxel size of $1.2 \times 1.2 \times 6\,mm^3$ translates into $8.6\,mm^3$ volume resolution, enabling sampling of small anatomical structures like hippocampus. Finally, we did not smooth images, and we used manually traced coregistered ROIs, which contributed to the reliability of hippocampal assessment.

This study had several limitations. We calibrated the tagged and untagged signal with WM. Although there is a potential bias due to WM disease, especially in subjects with high FCRP, the estimated low rates of WM perfusion are less than the increased *CBF* variability associated with uncorrected flow. Second, based on the segmentation procedure, all WM voxels containing < 75% of WM (see below) are removed from the WM ROI, which is used to correct cortical flow. We believe this reduced the WM disease-related bias.

Arterial stenosis is known to reduce both the *CBF* (Bokkers *et al*, 2009) and the capacity to respond to hypercapnia (Bricic *et al*, 2008; Markus and Harrison, 1992). However, most of the studies examined this issue in patients with symptomatic stenosis. None of our subjects fell into this category. Nonetheless, we cannot account for the influence

of stenotic lesions, as such information was not available. The prevalence of asymptomatic carotid stenosis ranges from 0.5% in people under 60 to up to 10% in subjects over the age of 80 years (Benavente *et al*, 1998). Stenosis is more common among patients with hypertension with prevalence reported to reach 25% (Sutton-Tyrrell *et al*, 1993). With a mean age of around 70 years and about 40% of subjects meeting criteria for hypertension, we can estimate that the probable prevalence of asymptomatic carotid stenosis in our group could not be higher than 5% to 10%. We consider it unlikely that this will affect our results.

The circulatory response to hypercapnia consists of increases in heart rate and arterial pressure. Unfortunately, we were not able to record blood pressure measurements during rebreathing procedure. For few reasons, we do not believe that these phenomena could significantly affect the results. First, hypercapnia induced during our study can be classified as mild. Second, heart rate (positively correlated with blood pressure) increased during the rebreathing challenge only by few percent.

Finally, the group with missing VR_h data could also represent a bias. These subjects had lower MMSE, pointing out to possible challenges in planning the study with impaired individuals. Our sample was small and perfusion was examined only in one slab. However, the hippocampus appeared to be sampled consistently in each case, because of careful slice positioning technique.

In conclusion, vascular risk, as measured with *FCRP*, correlates with both hippocampal and cortical vessels' ability to expand in response to a mild hypercapnia. The VR_h is more sensitive to vascular burden than either resting *CBF* or brain volume. It is compromised already in the MCI stage but vascular risk does not fully explain this impairment. It remains to be determined in longitudinal design how these effects contribute to cognitive deterioration. Further evaluation with bigger cohort, larger brain coverage, and more extensive assessment of vascular risk is crucial.

Acknowledgements

The authors thank Ms. Anna Hemraj for her assistance with study coordination.

Disclosure/conflict of interest

The authors declare no conflict of interest.

References

Ashburner J, Friston KJ (2000) Voxel-based morphometry–the methods. *Neuroimage* 11:805–21

Bakker SLM, de Leeuw FE, de Groot JC, Hofman A, Koudstaal PJ, Breteler MMB (1999) Cerebral vasomotor reactivity and cerebral white matter lesions in the elderly. *Neurology* 52:578

Beason-Held LL, Moghekar A, Zonderman AB, Kraut MA, Resnick SM (2007) Longitudinal changes in cerebral blood flow in the older hypertensive brain. *Stroke* 38:1766–73

Benavente O, Moher D, Pham B (1998) Carotid endarterectomy for asymptomatic carotid stenosis: a metaanalysis. *Br Med J* 317:1477–80

Bokkers RPH, van der Worp HB, Mali WPTM, Hendrikse J (2009) Noninvasive MR imaging of cerebral perfusion in patients with a carotid artery stenosis. *Neurology* 73:869–75

Bonoczk P, Panczel G, Nagy Z (2004) Vasoreactivity in patients with periventricular white matter lucency. *Acta Neurologica Scandinavica* 110:254–9

Boss A, Martirosian P, Klose U, Nagele T, Claussen CD, Schick F (2007) FAIR-TrueFISP imaging of cerebral perfusion in areas of high magnetic susceptibility differences at 1.5 and 3 Tesla. *J Magn Reson Imaging* 25:924–31

Bricic I, Horner S, Thaler D, Demarin V, Klein GE, Niederkorn K (2008) Improved cerebral vasoreactivity following percutaneous transluminal angioplasty with stenting of high-grade internal carotid artery stenosis. *Cerebrovasc Dis* 25:555–60

Buxton RB (2005) Quantifying CBF with arterial spin labeling. *J Magn Reson Imaging* 22:723–6

Caroli A, Testa C, Geroldi C, Nobili F, Barnden LR, Guerra UP, Bonetti M, Frisoni GB (2007) Cerebral perfusion correlates of conversion to Alzheimer's disease in amnestic mild cognitive impairment. *J Neurol* 254:1698–707

Chao LL, Buckley ST, Kornak J, Schuff N, Madison C, Yaffe K, Miller BL, Kramer JH, Weiner MW (2010) ASL perfusion MRI predicts cognitive decline and conversion from MCI to dementia. *Alzheimer Dis Assoc Dis* 24:19–27

Claus JJ, Breteler MMB, Hasan D, Krenning EP, Bots ML, Grobbee DE, van Swieten JC, van Harskamp F, Hofman A (1996) Vascular risk factors, atherosclerosis, cerebral white matter lesion and cerebral perfusion in a population based study. *Eur J Nucl Med* 23:675–82

Convit A, de Leon MJ, Tarshish C, De Santi S, Tsui W, Rusinek H, George AE (1997) Specific hippocampal volume reductions in individuals at risk for Alzheimer's disease. *Neurobiol Aging* 18:131–8

Dai W, Lopez OL, Carmichael OT, Becker JT, Kuller LH, Gach HM (2008) Abnormal regional cerebral blood flow in cognitively normal elderly subjects with hypertension. *Stroke* 39:349–54

Dai W, Lopez OL, Carmichael OT, Becker JT, Kuller LH, Gach HM (2009) Mild cognitive impairment and Alzheimer disease: patterns of altered cerebral blood flow at MR imaging. *Radiology* 250:856–66

Eichenbaum H (2004) Hippocampus: cognitive processes and neural representations that underlie declarative memory. *Neuron* 44:109–20

Fazekas F, Chawluk JB, Alavi A, Hurtig HI, Zimmerman RA (1987) MR signal abnormalities at 1.5 T in Alzheimer's dementia and normal aging. *Am J Roentgenol* 149:351–6

Folstein M (1983) The Mini-Mental State Examination. In *Assessment in Geriatric Psychopharmacology* (Crook T, Ferris SH, Bartus R eds), New Canaan: Mark Powley Associates pp 47–51

Fu JH, Lu CZ, Hong Z, Dong Q, Ding D, Wong KS (2006) Relationship between cerebral vasomotor reactivity and

white matter lesions in elderly subjects without large artery occlusive disease. *J Neuroimaging* 16:120–5

Glodzik-Sobanska L, Rusinek H, Mosconi L, Li Y, Zhan J, De Santi S, Convit A, Rich KE, Brys M, de Leon MJ (2005) The role of quantitative structural imaging in the early diagnosis of Alzheimer's disease. *Neuroimaging Clin N Am* 15:803–26

Groschel K, Terborg C, Riecker A, Witte OW, Kastrup A (2007) Effects of physiological aging and cerebrovascular risk factors on the hemodynamic response to brain activation: a functional transcranial Doppler study. *Clin Neurophysiol* 118:e35–6

Hansson O, Buchhave P, Zetterberg H, Blennow K, Minthon L, Warkentin S (2009) Combined rCBF and CSF biomarkers predict progression from mild cognitive impairment to Alzheimer's disease. *Neurobiol Aging* 30:165–73

Hirao K, Ohnishi T, Hirata Y, Yamashita F, Mori T, Moriguchi Y, Matsuda H, Nemoto K, Imabayashi E, Yamada M, Iwamoto T, Arima K, Asada T (2005) The prediction of rapid conversion to Alzheimer's disease in mild cognitive impairment using regional cerebral blood flow SPECT. *Neuroimage* 28:1014–21

Ijzerman RG, de Jongh RT, Beijk MAM, van Weissenbruch MM, Delemarre-van De Waal HA, Serne EH, Stehouwer CD (2003) Individuals at increased coronary heart disease risk are characterized by an impaired microvascular function in skin. *Eur J Clin Invest* 33:536–42

Isaka Y, Okamoto M, Ashida K, Imaizumi M (1994) Decreased cerebrovascular dilatory capacity in subjects with asymptomatic periventricular hyperintensities. *Stroke* 25:375–81

Johnson KA, Jones K, Holman BL, Becker BS, Spiers PA, Satlin A, Albert MS (1998) Preclinical prediction of Alzheimer's disease using SPECT. *Neurology* 50: 1563–71

Kitagawa T, Oku N, Kimura Y, Yagita Y, Sakaguchi M, Hatazawa J, Sakoda S (2009) Relationship between cerebral blood flow and later cognitive decline in hypertensive patients with cerebral small vessel disease. *Hypertension Res* 32:816–20

Last D, de Bazelaire C, Alsop DC, Hu K, Abduljalil AM, Cavallerano J, Marquis RP, Novak V (2007) Global and regional effects of type 2 diabetes on brain tissue volumes and cerebral vasoreactivity. *Diabetes Care* 30:1193–9

Law I, Iida H, Holm S, Nour S, Rostrup E, Svarer C, Paulson OB (2000) Quantitation of regional cerebral blood flow corrected for partial volume effect using O-15 water and PET: II. Normal values and gray matter blood flow response to visual activation. *J Cerbral Blood Flow Metab* 20:1237–51

Markus HS, Harrison MJ (1992) Estimation of cerebrovascular reactivity using transcranial Doppler, including the use of breath-holding as the vasodilatory stimulus. *Stroke* 23:668–73

Mosconi L (2005) Brain glucose metabolism in the early and specific diagnosis of Alzheimer's disease. *Eur J Nucl Med* 32:486–510

Mosconi L, Tsui WH, De Santi S, Rusinek H, Li J, Convit A, Li Y, de Leon MJ (2005) Reduced hippocampal metabolism in mild cognitive impairment and Alzheimer's disease: automated FDG-PET image analysis. *Neurology* 64:1860–7

NIH Publication No.02-5125 & US Department of Health and HUman Services, N.I.o.H.N.H.L.a.B.I (2002) Third report of the National Cholesterol Education Program (NCEP) expert panel on detection, evaluation and treatment of high cholesterol in adults (Adult Treatment panel III) final report. *Circulation* 106:3143

Novak V, Last D, Alsop DC, Abduljalil AM, Hu K, Lepicovsky L, Cavallerano J, Lipsitz LA (2006) Cerebral blood flow velocity and periventricular white matter hyperintensities in type 2 diabetes. *Diabetes Care* 29:1529–34

Petersen ET, Zimine I, Ho Y-CL, Golay X (2006) Non-invasive measurement of perfusion: a critical review of arterial spin labelling techniques. *Br J Radiol* 79:688–701

Reisberg B, Ferris SH (1988) The brief cognitive rating scale (BCRS) psychopharmacology. *Bulletin* 24:629–36

Reisberg B, Sclan SG, Franssen EH, de Leon MJ, Kluger A, Torossian CL, Shulman E, Steinberg G, Monteiro I, McRae T, Boksay I, Mackell JA, Ferris SH (1993) Clinical stages of normal aging and Alzheimer's disease: the GDS staging system. *Neurosci Res Commun* 13(Suppl 1):551–4

Rusinek H, Glodzik L, Brys M, Haas F, Mcgorty KA, Chen Q, de Leon MJ (2010) *Hippocampal Blood Flow and Vascular Reactivity in Normal Aging*. Proceedings of the 18th scientific meeting ISMRM, Stockholm, Sweden, 1–7 May

Sandor P, De Jong W, De Wied D (1986) Endorphinergic mechanisms in cerebral blood flow autoregulation. *Brain Res* 386:122–9

Selim M, Jones R, Novak P, Zhao P, Novak V (2008) The effects of body mass index on cerebral blood flow velocity. *Clin Auton Res* 18:331–8

Settakis G, Pall D, Molnar C, Bereczki D, Csiba L, Fulesdi B (2003) Cerebrovascular reactivity in hypertensive and healthy adolescents: TCD with vasodilatory challenge. *J Neuroimaging* 13:106–12

Shapiro M (2001) Plasticity, hippocampal place cells, and cognitive maps. *Arch Neurol* 58:874–81

Silvestrini M, Pasqualetti P, Baruffaldi R, Bartolini M, Handouk Y, Matteis M, Moffa F, Provinciali L, Vernieri F (2006) Cerebrovascular reactivity and cognitive decline in patients with Alzheimer disease. *Stroke* 37:1010–5

Sparks DL, Scheff SW, Liu H, Landers TM, Coyne CM, Hunsaker JCI (1995) Increased incidence of neurofibrillary tangles (NFT) in non-demented individuals with hypertension. *J Neurol Sci* 131:162–9

Staffen W, Schonaueer U, Zauner H, Spindler I, Mair A, Iglseder B, Bernroider G, Ladurner G (2006) Brain perfusion SPECT in patients with mild cognitive impairment and Alzheimer's disease: comparison of a semiquantitative and a visual evaluation. *J Neural Trans* 113:195–203

Stanisz GJ, Odrobina EE, Pun J, Escaravage M, Graham SJ, Bronskill MJ, Henkelman RM (2005) T1, T2 relaxation and magnetization transfer in tissue at 3T. *Magn Resonance Med* 54:507–12

Sutton-Tyrrell K, Alcorn HG, Wolfson Jr SK, Kelsey SF, Kuller LH (1993) Predictors of carotid stenosis in older adults with and without isolated systolic hypertension. *Stroke* 24:355–61

Vincenzini E, Ricciardi MC, Altieri M, Puccinelli F, Bonaffini N, Di Piero V, Lenzi GL (2007) Cerebrovascular reactivity in degenerative and vascular dementia: a transcranial Doppler study. *Eur Neurol* 58:84–9

Zarow C, Vinters HV, Ellis WG, Weiner MW, Mungas D, White L, Chui HC (2005) Correlates of hippocampal neuron number in Alzheimer's disease and ischemic vascular dementia. *Ann Neurol* 57:896–903